applied sciences

MDPI

Article

Transverse Crack Behavior in Continuously Reinforced Concrete Pavement with Basalt Fiber Reinforcement

Yating Zhang [1,*] and Zhiyi Huang [2]

[1] School of Environmental and Civil Engineering, Jiangnan University, Wuxi 214122, China
[2] College of Civil Engineering and Architecture, Zhejiang University, Hangzhou 310058, China; hzy@zju.edu.cn
* Correspondence: ytzhang@jiangnan.edu.cn; Tel.: +86-0510-8591-2822

Received: 1 October 2020; Accepted: 21 October 2020; Published: 23 October 2020



Abstract: Continuously reinforced concrete pavement (CRCP) is a pavement structure with a high performance and long service life. However, the corrosion of the longitudinal steel can result in a poor bond relationship between the steel and the concrete, affecting the load transfer efficiency between the adjacent panels and being responsible for the development of CRCP distresses. Basalt fiber-reinforced polymer (BFRP) is corrosion-resistant and has the potential to be used in CRCP. In this paper, the layout of a CRCP test section with BFRP bars constructed on G330 National Road in Zhejiang Province, China, is presented. An analytical model is proposed to predict the crack behavior of CRCP with BFRP reinforcement, with the predicted results are compared to field-measured ones. A sensitivity analysis of the BFRP design parameters on the crack spacing and crack width is conducted as well. The results show that the mean values for field-measured crack spacing and crack width are 4.85 m and 1.30 mm, respectively, which are higher than the results for traditional CRCP with steel due to the lower elastic modulus of BFRP. The analytical predictions agree reasonably well with the crack survey results. The higher the elastic modulus of BFRP, the reinforcement content (with both BFRP spacing and diameter related), and the bond stiffness coefficient between the BFRP and concrete, the less the crack spacing and crack width will be. Given the same or similar reinforcement content, a lower diameter with a smaller spacing is recommended because of its contribution to a smaller crack spacing and width.

Keywords: continuously reinforced concrete pavement (CRCP); basalt fiber-reinforced polymer (BFRP); transverse crack behavior; field survey; analytical model

1. Introduction

Continuously reinforced concrete pavement (CRCP) is a high-performance pavement structure that requires minimal maintenance while maintaining its smoothness over time. The closely distributed transverse crack pattern in CRCP reduces stresses in the slab, and the combination of tight cracks and steel reinforcement maintains a relatively high degree of stiffness, which allows for a resistant structural system and a high ride quality.

For traditional CRCP, steel is the most common material for longitudinal reinforcement. However, the corrosive property of steel can significantly reduce the bond stiffness of the steel and concrete, causing a decrease in the load transfer efficiency and aggregate interlock between the adjacent concrete slabs, therefore widening the crack width, which is an important indicator for CRCP performance [1,2]. There have been many studies evaluating the crack behavior and structural performance of CRCP [3–9], indicating that the aggregate type, the reinforcement content and depth, the slab-base friction, and the

environmental load, etc., have great effect on the crack spacing and crack width and, as a result, affect the structural performance of the CRCP.

Recently, corrosion-resistant materials such as glass fiber-reinforced polymer (GFRP) [10] have been proposed as an alternative longitudinal reinforcement in CRCP in order to improve the bond condition between the longitudinal reinforcement and concrete, thus achieving a better crack behavior in CRCP. The first CRCP with GFRP bars as both a longitudinal and transverse reinforcement was constructed in West Virginia and showed a good performance [11]. Based on the test section results, an overall design methodology for CRCP with GFRP bars was proposed [12]. Furthermore, an analytical model of a fully supported reinforced concrete panel was developed to describe the shrinkage and thermal stress distribution in CRCP with GFRP bars, demonstrating the relationship between the crack behavior and the CRCP design parameters [13]. In addition to West Virginia, a GFRP-CRCP test section was built in Canada as well, with GFRP bars as both longitudinal and transverse reinforcements since the corrosion of steel is one design criteria for the CRCP with a long service life [14]. Given the field results after six years of service under actual traffic conditions, the GFRP-CRCP test section in Canada was shown to provide a competitive performance in comparison to CRCP with steel bars [15].

Like GFRP, basalt fiber-reinforced polymer (BFRP) is also a promising alternative for steel in conventional CRCP due to its great corrosion-resistant characteristics and high tensile strength. Gu and Dong [16] have conducted a serious of pull-out tests to investigate the effect of various ribs and anchorage lengths on the bond performance of concrete and BFRP bars, with the test results verified with the finite element model, showing that a sufficient bond between BFRP and concrete can be achieved for CRCP. However, there are few case studies presenting the field performance of CRCP with BFRP reinforcements.

In this study, a 250 m-long CRCP test section with BFRP bars, built in Jinhua, Zhejiang Province, in China, was presented and the early crack behavior was studied. The research significance of this work was to evaluate the viability of using BFRP in CRCP sections as well as the reasonableness of the analytical cracking model. The crack spacing and crack width in the BFRP-CRCP test section was evaluated with both a field crack survey and the proposed analytical model. Furthermore, an evaluation of the effect of the BFRP design parameters, such as the elastic modulus of BFRP, the BFRP content, and the bond stiffness between the BFRP and the concrete, on the crack behavior was conducted to optimize the BFRP design for CRCP with BFRP bars.

2. Details of the CRCP Test Section with BFRP Bars

The test section is 250 m long, as part of an existing three-lane concrete pavement on the G330 National Road from K200 + 400 to K200 + 650 in Zhejiang Province in China. Each lane is nominally 4 m wide on a 2% longitudinal grade. The two inside lanes were chosen to be part of the test section, which were reconstructed with CRCP containing BFRP reinforcement, while the outer lane (jointed plain concrete pavement, JPCP) was used for traffic during reconstruction. A longitudinal contraction joint in the 8 m-wide lane was not part of the design or construction process. One month after the construction of the CRCP section, a 10 cm-thick HMA layer was placed on top of both the CRCP lanes and the existing outer lane. Temperature sensors and pressure and strain gages were adopted in this test section to monitor the early age behavior of the CRCP with BFRP bars.

The field CRCP test section was constructed in September 2014. A 15 cm-thick cement-stabilized subbase with 3% Portland cement and crushed stone was first constructed to provide uniform support. A 20 cm-thick cement-stabilized base with 5% Portland cement and crushed stone was then constructed next on top of the subbase. Next, a 26 cm-thick CRCP layer with a water/cement ratio of 0.38 given BFRP as both longitudinal and transverse reinforcement was constructed on top of the base layer, with a 6 cm-thick HMA binder layer given the nominal max aggregate size of 16 mm and a 4 cm-thick SBS-modified HMA layer given the nominal max aggregate size of 13 mm constructed one month after casting the CRCP layer. Between the CRCP and asphalt layer, there is a bonding layer consisting of 1 cm-thick SBS-modified asphalt with crushed stone distributed on it, casted a few hours before

the construction of the asphalt layer. The layout of the CRCP test section with BFRP reinforcement is presented in Figure 1.

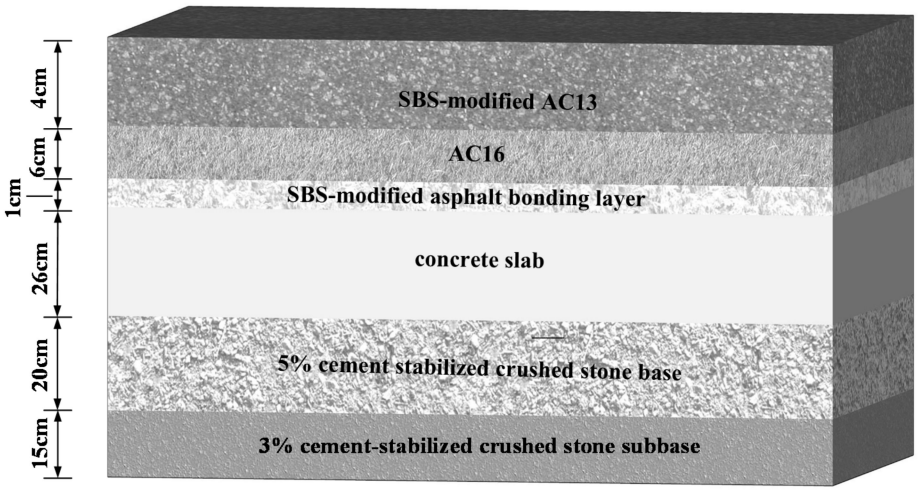


Figure 1. The layout of the continuously reinforced concrete pavement (CRCP) test section with basalt fiber-reinforced polymer (BFRP) bars.

The diameter of the longitudinal BFRP reinforcement was 12 mm, spaced at 8 cm with a reinforcement content of 0.50%, and placed at the mid-depth of the concrete slab—i.e., 13 cm deep from the top of the BFRP reinforcement to the CRCP surface. The diameter of longitudinal BFRP bars for this CRCP test section were smaller compared to traditional CRCPs with steel bars since the tensile strength of BFRP reinforcement is usually around 750 MPa, which is higher than the tensile strength of steel bars (550 MPa), while the elastic modulus of the BFRP reinforcement (40 GPa) is closer to that of concrete (30 GPa) than that of steel bars (210 GPa). As a result, a smaller bar size of the BFRP reinforcement can be used without significantly affecting the bond condition between the longitudinal reinforcement and the concrete. In addition, the diameter of the transverse BFRP reinforcements was 14 mm, spaced at 50 cm, and placed at a 30° angle to the horizontal (i.e., skewed), as shown in Figure 2. The material properties of the BFRP reinforcement were obtained from the manufacturer, and are compared to typical steel bars in Table 1.



Figure 2. The layout of the longitudinal BFRP reinforcement on transverse chairs.

Table 1. Geometric and mechanical properties of BFRP and steel reinforcement.

Parameters	Longitudinal BFRP Bars	Transverse BFRP Bars	Steel Bars
Diameter (mm)	12	14	-
Cross-Sectional Area (mm^2)	113.04	153.86	-
Elastic Modulus (GPa)	40	40	210
Tensile Strength (MPa)	750	750	550

3. Field Observation Results

3.1. Crack Behavior in the CRCP Layer

A total of three field surveys for the BFRP-reinforced CRCP layer were conducted in the first month, before the placement of the asphalt surface, with the first observation at 12 h after the casting of the slab, the second survey performed 12 days after concrete casting, and the third survey conducted 36 days after the construction. The mean values of the transverse crack spacing and crack width from each survey are summarized in Table 2, giving the crack spacings obtained using the distance measuring wheel and the crack widths recorded with a crack comparator.

Table 2. Mean values of the transverse crack spacing and width at different times.

	Crack Spacing (m)	Crack Width (mm)
12 h	-	-
12 days	6.22	0.95
36 days	4.85	1.30

Figure 3 shows the crack maps of the BFRP-reinforced CRCP test section based on each observational survey.

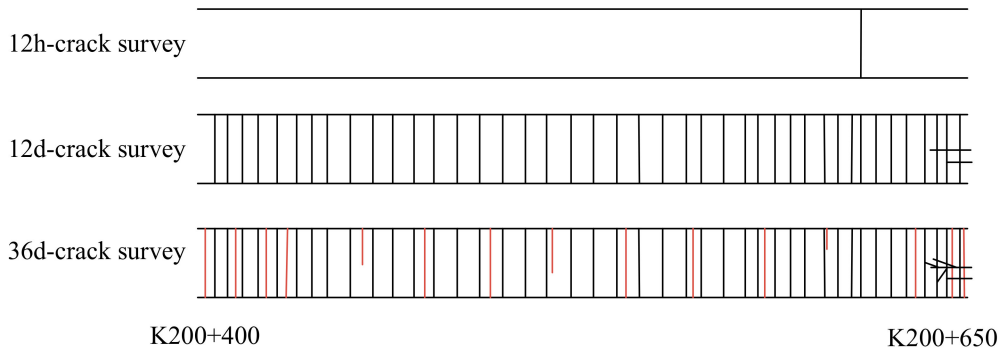


Figure 3. Crack maps of the BFRP-CRCP test section from crack surveys.

As shown in Figure 3, only one transverse crack was found near the end of the slab, with a crack width around 0.4 mm in the first survey. Many new transverse cracks appeared during the second crack survey, with the mean crack spacing and crack width of 6.22 m and 0.95 mm, respectively. Meanwhile, in the last survey, as expected, several new transverse cracks were found between the existing transverse cracks, with the new mean crack spacing and crack width developing to 4.85 m and 1.30 mm, respectively. As for the crack width, the new transverse crack appearing on the third survey were lower compared to those existing transverse cracks because of the greater concrete stiffness at later ages and shorter spacing between cracks.

3.2. Crack Behavior in Asphalt Layer

After finishing the asphalt overlay, a field observation was also conducted on 14 December 2014, 98 days after the slab casting and 61 days after the placement of the HMA overlay. The HMA composite

CRCP test section showed no transverse cracks except for the one at the end of the test section, where irregular cracks had appeared in the CRCP before placing the asphalt layer, as shown in Figure 4.



Figure 4. Irregular cracks in the CRCP (**left**) and transverse reflection crack in the asphalt layer (**right**).

In addition to the transverse crack, there is a longitudinal reflection crack in the HMA at the construction joint between the new CRCP lanes and existing JPCP. The irregular crack at the end of the concrete slab is likely responsible for the transverse reflection crack shown in the HMA. The appearance of the longitudinal reflection crack is because of the differential deflection at the construction joint between the newly constructed CRCP and the existing JPCP.

4. Analytical Analysis of the Transverse Cracks in BFRP-CRCP

4.1. Analytical Model for BFRP-CRCP

Both the friction between the concrete and the base layer and the bond between the concrete and the BFRP reinforcement impose a constraint on the concrete horizontal displacement, and thus friction and bond must be introduced into the analytical model to predict crack spacing and crack width [17]. It was assumed that the friction-slip relationship between the base and the concrete as well as bond-slip relationship between the BFRP reinforcement and the concrete are linear, as shown in Equations (1) and (2).

$$\tau_c = k_c u_c, \tag{1}$$

$$\tau_s = k_s(u_c - u_s), \tag{2}$$

where τ_c is the frictional stress between the concrete and the base layer; τ_s is the bond stress between the BFRP reinforcement and the concrete; u_c and u_s are the displacement of the concrete and the BFRP reinforcement, respectively; k_c is the friction coefficient between the concrete slab and the base layer; and k_s is the bond-slip coefficient between the concrete and the BFRP reinforcement. A schematic of the analytical model is shown in Figure 5.

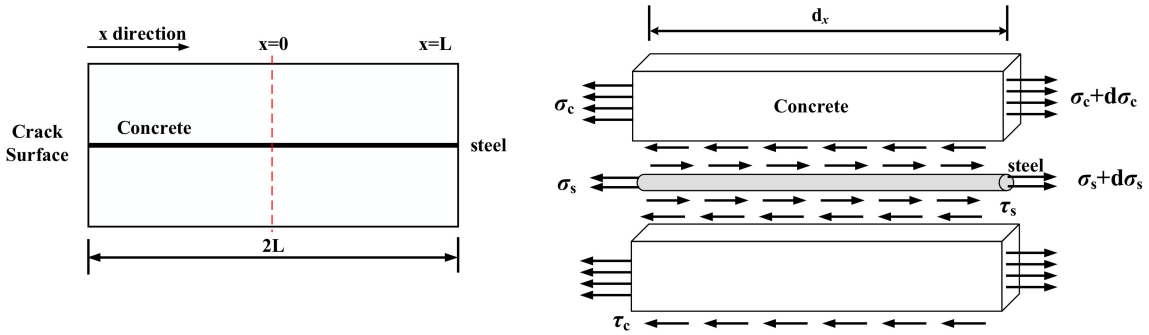


Figure 5. Analytical model for BFRP-CRCP (2 L is crack spacing).

Based on force equilibrium equations of the concrete and the BFRP reinforcement and the stress–strain relationship of the concrete and the BFRP reinforcement, Equations (3)–(6) can be obtained.

$$\frac{\mathrm{d}\sigma_c}{\mathrm{d}x} - \frac{\pi d_s}{A_c}\tau_s - \frac{b}{A_c}\tau_c = 0, \tag{3}$$

$$\frac{\mathrm{d}\sigma_s}{\mathrm{d}x} + \frac{\pi d_s}{A_c}\tau_s = 0, \tag{4}$$

$$\sigma_c = E_c\varepsilon_c = E_c\left(\frac{\mathrm{d}u_c}{\mathrm{d}x} - \alpha_c\Delta T - \varepsilon_{sh}\right), \tag{5}$$

$$\sigma_s = E_s\varepsilon_s = E_s\left(\frac{\mathrm{d}u_s}{\mathrm{d}x} - \alpha_s\Delta T\right), \tag{6}$$

where σ_c and σ_s are the stress of the concrete and the BFRP reinforcement, respectively; E_c and E_s are the elastic modulus of the concrete and the BFRP reinforcement, respectively; α_c and α_s are the linear expansion coefficients of the concrete and the BFRP reinforcement, respectively; A_c is the cross sectional area of the concrete; d_s is the diameter of the BFRP reinforcement; b is the spacing of the BFRP reinforcement; ε_{sh} is the shrinkage of the concrete; and ΔT is the mean pavement temperature drop from the temperature during concrete casting to coldest temperature in the year 2014 in the test section area. Next, u_c and u_s can be expressed in Equations (7) and (8):

$$\frac{\mathrm{d}^2u_c}{\mathrm{d}x^2} - (a_1 + a_2)u_c + a_1u_s = 0, \tag{7}$$

$$\frac{\mathrm{d}^2u_s}{\mathrm{d}x^2} - a_3u_s + a_3u_c = 0, \tag{8}$$

where a_i is indicated in Equations (9)–(11).

$$a_1 = \frac{\pi d_s k_s}{A_c E_c}, \tag{9}$$

$$a_2 = \frac{bk_c}{A_c E_c}, \tag{10}$$

$$a_3 = \frac{\pi d_s k_s}{A_s E_s}. \tag{11}$$

In order to obtain the solutions for the displacement and stress of the concrete and the BFRP reinforcement, four boundary conditions were proposed, assuming that the displacement of the BFRP reinforcement and the stress of the concrete are zero at the concrete crack surface (x = L), while the displacement of both the BFRP reinforcement and concrete are zero at the mid-slab section (x = 0). By solving ordinary differential equations at these boundary conditions, u_c and u_s can be calculated in Equations (12) and (13), respectively, and σ_c and σ_s can be obtained from Equations (14) and (15).

$$u_c = C_1(e^{r_1x} - e^{-r_1x}) + C_2(e^{r_2x} - e^{-r_2x}), \tag{12}$$

$$u_s = C_1b_1(e^{r_1x} - e^{-r_1x}) + C_2b_2(e^{r_2x} - e^{-r_2x}), \tag{13}$$

$$\sigma_c = E_c(C_1r_1(e^{r_2x} + e^{-r_2x}) + C_2r_2(e^{r_2x} + e^{-r_2x}) - \alpha_c\Delta T - \varepsilon_{sh}), \tag{14}$$

$$\sigma_s = E_s(C_1b_1r_1(e^{r_1x} + e^{-r_1x}) + C_2b_2r_2(e^{r_2x} + e^{-r_2x}) - \alpha_s\Delta T), \tag{15}$$

where C_i, r_i, and b_i are defined in Equations (16)–(21):

$$C_1 = \frac{(\alpha_c\Delta T + \varepsilon_{sh})b_2\left(e^{r_2L} - e^{-r_2L}\right)}{b_1r_2\left(e^{-r_1L}e^{r_2L} - e^{r_1L}e^{-r_2L} - e^{r_1L}e^{r_2L} + e^{-r_1L}e^{-r_2L}\right) + b_2r_1\left(e^{r_1L}e^{r_2L} - e^{-r_1L}e^{-r_2L} - e^{r_1L}e^{-r_2L} + e^{-r_1L}e^{r_2L}\right)}, \tag{16}$$

$$C_2 = \frac{-(\alpha_c \Delta T + \varepsilon_{sh}) b_1 \left(e^{r_1 L} - e^{-r_1 L}\right)}{b_1 r_2 \left(e^{-r_1 L} e^{r_2 L} - e^{r_1 L} e^{-r_2 L} - e^{r_1 L} e^{r_2 L} + e^{-r_1 L} e^{-r_2 L}\right) + b_2 r_1 \left(e^{r_1 L} e^{r_2 L} - e^{-r_1 L} e^{-r_2 L} - e^{r_1 L} e^{-r_2 L} + e^{-r_1 L} e^{r_2 L}\right)}, \quad (17)$$

$$r_1 = \sqrt{\frac{1}{2}\left(a_1 + a_2 + a_3 + \sqrt{(a_1 + a_2 + a_3)^2 - 4a_2 a_3}\right)}, \quad (18)$$

$$r_2 = \sqrt{\frac{1}{2}\left(a_1 + a_2 + a_3 - \sqrt{(a_1 + a_2 + a_3)^2 - 4a_2 a_3}\right)}, \quad (19)$$

$$b_1 = \frac{\left(a_1 + a_2 - r_1^2\right)}{a_1}, \quad (20)$$

$$b_2 = \frac{\left(a_1 + a_2 - {r_2}^2\right)}{a_1}. \quad (21)$$

The concrete was assumed to produce a transverse crack with a certain crack width when the concrete stress reaches the tensile strength of the concrete, and therefore the final crack spacing (C_S) of the CRCP can be obtained by determining the length of the CRCP slab that produces an equivalent tensile stress to the concrete tensile strength, as shown in Equations (22) and (23).

$$\sigma_{c-max} = \sigma_c\big|_{x=0} = f_t, \quad (22)$$

$$C_S = 2L, \quad (23)$$

where f_t is the tensile strength of the concrete material. Crack width (C_W) can be obtained by calculating this critical slab length from Equations (23) and (24).

$$C_W = 2u_c|_{x=L}. \quad (24)$$

4.2. Analytical Results

Table 3 presents the input parameters of the concrete and the BFRP for obtaining the analytical predictions. All the geometric parameters of the concrete and BFRP—i.e., the thickness of the concrete, the BFRP diameter, the reinforcement ratio of BFRP, and the spacing of BFRP—were the same as those specified in the aforementioned CRCP test section with BFRP bars. The concrete material properties were from the results of the lab tests. The coefficient of the bond stiffness of the BFRP and the concrete was calculated through pull-out test results of the concrete and BFRP bars, while the friction coefficient between the concrete and the base layer and the linear expansion coefficient of the BFRP reinforcement were estimated based on a previous study [18]. ΔT was the temperature drop from the temperature during concrete casting to the coldest temperature in the year 2014 in the test section area.

Table 3. Input parameters for the BFRP-CRCP test section for the analytical model.

Parameters	Concrete	BFRP
Elastic Modulus (GPa)	30	40
Tensile Strength (MPa)	3.20	750
Compressive Strength (MPa)	40	-
Concrete Shrinkage	0.0002	-
Coefficient of Linear Expansion (10^{-6}/°C)	10	9
Thickness of CRCP (cm)	26	-
Reinforcement content (%)		0.50
ΔT (°C)	30	-
Coefficient of Friction (MPa/m)	40	-
Coefficient of Bond Stiffness (GPa/m)	-	30
BFRP Diameter (mm)	-	12
BFRP Spacing (cm)	-	8

Based on the inputs in Table 3, the analytical predictions for the crack spacing and crack width in CRCP with BFRP bars were calculated to be 4.47 m and 1.78 mm, respectively, as described in Figure 6. The greater crack spacing and width for the BFRP is mainly due to the lower elastic modulus of BFRP, which is 40 GPa as compared to the steel (210 GPa). In order to achieve a lower crack spacing and crack width in CRCP with BFRP reinforcement, one possible way is to increase the reinforcement ratio of the BFRP bar.

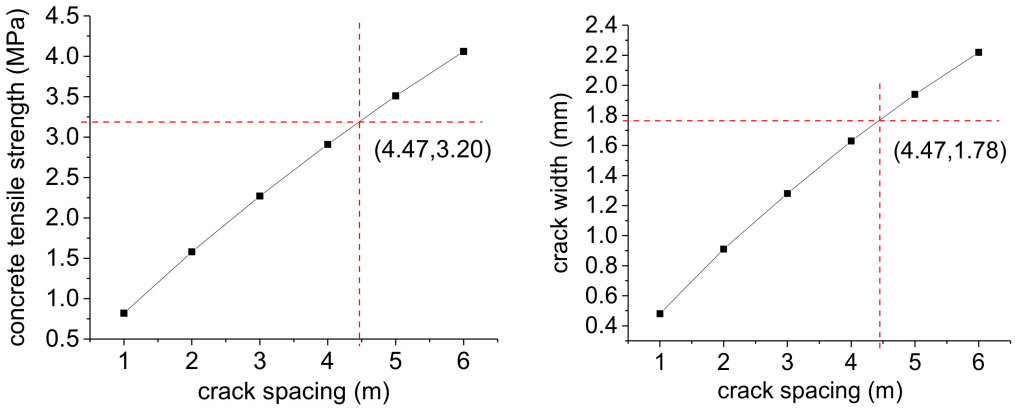


Figure 6. Predictions of the crack spacing (**left**) and crack width (**right**) in CRCP with BFRP bars.

4.3. Comparison and Analysis

The field observation and analytical calculation results for both the crack spacing and crack width of CRCP with BFRP bars without an asphalt overlay are presented in Table 4.

Table 4. Comparison of the field-measured and predicted crack spacing and crack width.

	Crack Spacing (m)	Crack Width (mm)
Final field observation	4.85	1.30
Analytical results	4.47	1.78

As for the crack spacing, the result of the analytical calculation was 4.47 m, which is less than but close to the field observation result. Meanwhile, for crack width the analytical result was 1.78 mm, a little higher than the field measured one (1.30 mm). Theoretically, this difference can be produced by the assumption of the linear bond–slip relationship between the concrete and the BFRP reinforcement, and the friction between the concrete slab and the base. Furthermore, the differential moisture and temperature effects in the field that are not included in the model, which can cause differences in the prediction results and the field-measured ones as well. In addition to the theoretical explanations, the transverse cracks in CRCP develop with time and tend to be fully developed in around two to three years, according to the field surveys from McGhee [19]. However, the crack survey of this CRCP test section with BFRP reinforcement is only conducted as long as 36 days after the construction and, therefore, the field-measured results must be lower than the prediction values, which are normally used to estimate the final crack spacing and crack width for the CRCP. In general, a reasonable agreement was achieved from the field observations and analytical calculations, with a slight overprediction of crack spacing and crack width at earlier ages occurring in the model.

For traditional CRCP with steel bars, the transverse crack spacing usually ranges from 1.2 to 1.8 m [20,21] with a crack width less than 0.5 mm, which is suggested in the American Association of State Highway and Transportation Officials (AASHTO) standard [22]. However, since the corrosion resistant property of the BFRP reinforcement, a less harsh requirement for crack width in CRCP with BFRP bars can be accepted. To provide a better performance for the CRCP structure, the influence of the BFRP design parameters (the elastic modulus, the reinforcement content of BFRP bars (both BFRP

spacing and diameter-related), and the coefficient of bond stiffness between the concrete and the BFRP reinforcement) on the transverse crack behavior of CRCP needs to be thoroughly investigated.

5. Impact of BFRP Design Parameters on Transverse Crack Behavior of CRCP

5.1. Elastic Modulus of BFRP

Figure 7 presents the analytical results of the effect of elastic modulus of BFRP on the crack spacing and crack width of CRCP. It can be illustrated that both the crack spacing and crack width are significantly affected by the elastic modulus of BFRP given a decrease of 27.7% and 27.5% in crack spacing and crack width, respectively, when the elastic modulus of BFRP increases from 40 to 80 GPa. This indicates that the low elastic modulus is responsible for the larger crack spacing and crack width in the CRCP with BFRP bars, and increasing the elastic modulus of BFRP can effectively reduce the crack spacing and width of CRCP. Since the crack width is a dominant indicator for the evaluation of CRCP performance, the selection of a reinforcement with a higher elastic modulus is very important to the performance of CRCP.

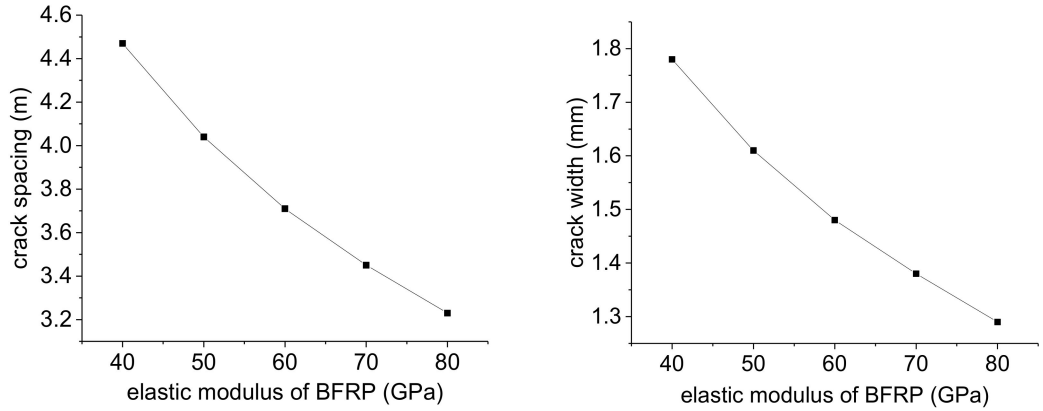


Figure 7. Impact of elastic modulus of BFRP on the crack spacing (**left**) and crack width (**right**) of CRCP with BFRP bars.

5.2. Reinforcement Content of BFRP

The variation in reinforcement content of BFRP can be related to both the bar spacing and diameter of BFRP. The influence of the bar spacing and diameter of BFRP on crack spacing and crack width are shown in Figures 8 and 9, respectively. As described in Figure 8, the more the spacing of the BFRP, the higher the crack spacing and crack width of CRCP. When the bar spacing increases from 6 to 14 cm, the crack spacing experiences a serious increase from 3.43 to 7.18 m, while the crack width increases sharply as well, from 1.36 to 2.87 mm. This can be attributed to the decrease in the reinforcement content of the BFRP bar. Given the bar spacing ranging from 6 to 14 cm, the corresponding reinforcement content decreases from 0.72% to 0.31%. Therefore, in order to achieve a lower crack spacing and crack width of CRCP, a reasonable bar spacing of BFRP needs to be carefully considered.

As expected, the diameter of BFRP bars also has great impact on both of the crack spacing and the crack width, with the higher the BFRP diameter, the lower the crack spacing and crack width of CRCP, as shown in Figure 9. Given an increase in the BFRP diameter from 10 to 18 mm, the corresponding reinforcement ratio of BFRP increases from 0.38% to 1.2%, resulting in a decrease of 55.9% (from 5.69 to 2.51 m) and 55.5% (from 2.27 to 1.01 mm) for crack spacing and crack width, respectively. Therefore, a rational increase in the BFRP diameter is an effective way to reduce the crack spacing and width of the CRCP with BFRP bars.

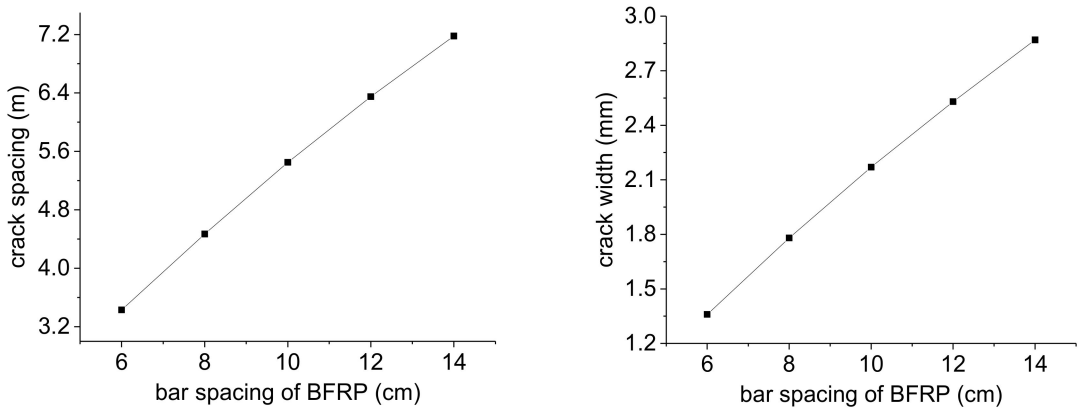


Figure 8. Impact of BFRP spacing on the crack spacing (**left**) and crack width (**right**) of CRCP with BFRP bars.

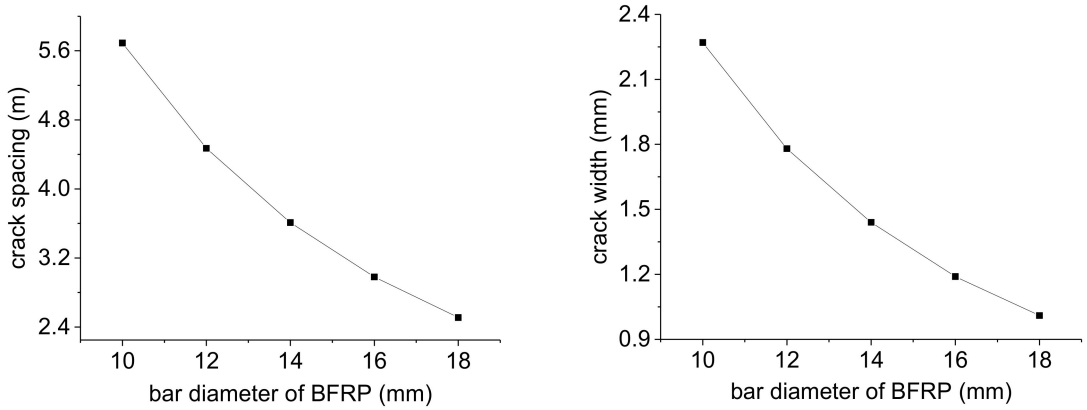


Figure 9. Impact of BFRP diameter on the crack spacing (**left**) and crack width (**right**) of CRCP with BFRP bars.

With the aforementioned range of BFRP spacing (6, 8, 10, 12, and 14 cm) and BFRP diameter (10, 12, 14, 16, and 18 mm), the reinforcement content for each combination of spacing and diameter can be calculated within the range of 0.22% to 1.63%. The relationship between the reinforcement content of BFRP and the crack spacing and width are presented in Figure 10. In general, both the crack spacing and crack width show a significant drop with an increase in the reinforcement content of BFRP bars. Since the reinforcement content is related to both the spacing and diameter of BFRP, the impact of different bar spacing and diameter given the same or similar reinforcement content on crack spacing and crack width was conducted to optimize the BFRP design in CRCP with BFRP bars.

Table 5 summarizes a similar reinforcement content with various combinations of BFRP spacings and diameters as well as the results of the crack spacing and width in CRCP with BFRP bars. Given reinforcement contents of 0.30% and 0.31%, the smaller BFRP spacing and BFRP diameter (10 cm and 10 mm, respectively) produced a lower crack spacing and width compared to the combination of 14 cm spacing and 12 mm diameter of BFRP. Interestingly, this relationship can also be found in reinforcement contents around 0.42%, 0.50%, 0.75%, and 0.98%, as presented in Table 5, indicating that closely spaced BFRP with a lower bar diameter can result in a lower crack spacing and crack width, given a similar reinforcement content of BFRP. For CRCP, a wider crack width is one of the distresses and is a key factor in the development of punchout. Therefore, given the same or similar reinforcement ratio, a smaller BFRP spacing and BFRP diameter are recommended to achieve better CRCP performance because of its contribution to the lower crack spacing and crack width.

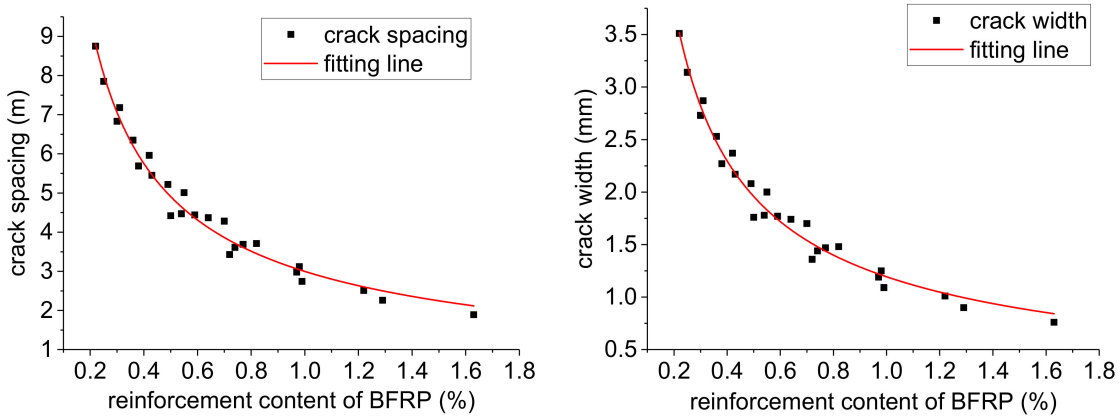


Figure 10. Impact of the reinforcement content of BFRP on the crack spacing (**left**) and crack width (**right**) of CRCP with BFRP bars.

Table 5. The impact of s similar reinforcement content with different bar spacing and diameter on the crack behavior of CRCP with BFRP bars.

Reinforcement Content (%)	Bar Spacing (cm)	Bar Diameter (mm)	Crack Properties	
			Spacing (m)	Width (mm)
0.30	10	10	6.83	2.73
0.31	14	12	7.18	2.87
0.42	14	14	5.96	2.37
0.43	10	12	5.45	2.17
0.49	12	14	5.22	2.08
0.50	6	10	4.42	1.76
0.74	8	14	3.61	1.44
0.77	10	16	3.69	1.47
0.97	8	16	2.98	1.19
0.99	6	14	2.74	1.09

5.3. Coefficient of Bond Stiffness of BFRP

Figure 11 shows the relationship between the coefficient of bond stiffness of BFRP and the transverse properties (crack spacing and crack width), given that the greater the coefficient of bond stiffness, the lower the crack spacing and crack width in CRCP. With the coefficient ranging from 20 to 60 GPa/m, the crack spacing decreases from 5.35 to 3.24 m while the crack width goes down from 2.13 to 1.29 mm, with both the crack spacing and width dropping by 39.4%. As a result, in order to provide good CRCP performance the bond stiffness between the BFRP and the concrete has to be guaranteed, which can be enhanced through increasing the surface thread depth and thread spacing of the BFRP reinforcement.

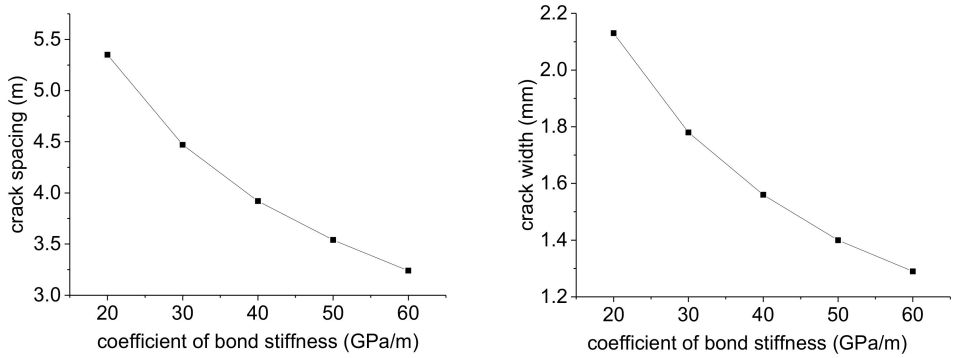


Figure 11. Impact of the coefficient of the bond stiffness of BFRP on the crack spacing (**left**) and crack width (**right**) of CRCP with BFRP bars.

6. Conclusions

BFRP reinforcement are corrosion-resistant and have the potential to be used in CRCP. A 250 m test section of CRCP with BFRP bars was constructed in Zhejiang Province in China. The transverse crack spacing and crack width in the test section after one month of construction was measured prior to the placement of the HMA overlay, with the mean field-measured values of 4.85 m and 1.30 mm for the crack spacing and crack width, respectively, which are higher than the results for the conventional CRCP with steel bars. This mainly due to the lower elastic modulus (40 GPa) of BFRP bars compared to steel bars (210 GPa). An analytical model was presented to predict the crack behavior in BFRP-CRCP, with the crack spacing and width of 4.47 m and 1.78 mm, respectively, overpredicting but reasonably agreeing with the field survey results, since a period of 36 days is not enough for the transverse crack to be fully developed. The BFRP design parameters have a significant impact on the crack spacing and crack width in BFRP-CRCP. The greater the elastic modulus, reinforcement content (both BFRP spacing and diameter-related), and bond stiffness coefficient of BFRP, the lower the crack spacing and crack width. Given that the elastic modulus of BFRP increases from 40 to 80 GPa; the BFRP spacing decreases from 14 to 6 cm; the BFRP diameter ranges from 8 to 16 mm; the coefficient of the BFRP bond stiffness increases from 20 to 60 GPa/m; the crack spacing experiences a drop of 27.7%, 52.2%, 55.9%, and 39.4%, respectively; and the crack width presents a drop of 27.5%, 52.6%, 55.5%, and 39.4%, respectively. Given the same or similar reinforcement content of BFRP, a lower bar diameter with a smaller spacing is recommended in order to achieve a smaller crack spacing and crack width in the CRCP. Further field observations of the CRCP with BFRP bars are still necessary, and the load transfer efficiency between adjacent slabs with BFRP bars needs to be conducted because of the larger crack width compared to that of conventional CRCP with steel bars.

Author Contributions: Conceptualization: Y.Z.; validation: Z.H. and Y.Z.; investigation: Y.Z.; methodology: Y.Z.; data curation: Y.Z.; supervision: Z.H.; writing—original draft preparation: Y.Z.; writing—review and editing: Y.Z. and Z.H. All authors have read and agreed to the published version of the manuscript.

Funding: This research was funded by the Natural Science Foundation of Jiangsu Province (BK20190604), Jiangsu Planned Projects for Postdoctoral Research Funds (2020Z327), Key Laboratory of Road and Traffic Engineering of the Ministry of Education, Tongji University (K202002), and the Fundamental Research Funds for the Central Universities (JUSRP11937).

Acknowledgments: The authors would like to acknowledge the support of Jeffery Roesler from the University of Illinois at Urbana-Champaign.

Conflicts of Interest: The authors declare no conflict of interest.

References

1. Jeon, S.I.; Choi, P.; Won, M. Punchout evaluations and classification of continuously reinforced concrete pavement to improve pavement design. *Road Mater. Pavement Des.* **2019**. [CrossRef]
2. Zollinger, D. Investigation of Punchout Distress in Continuously Reinforced Concrete Pavement. Ph.D. Thesis, University of Illinois, Urbana, IL, USA, 1989.
3. Oh, H.J.; Cho, Y.K.; Kim, S.M. Experimental evaluation of crack width movement of continuously reinforced concrete pavement under environmental load. *Constr. Build. Mater.* **2017**, *137*, 85–95. [CrossRef]
4. Kohler, E.; Roesler, J. Crack Width Measurements in Continuously Reinforced Concrete Pavements. *J. Transp. Eng.* **2005**, *131*, 645–652. [CrossRef]
5. Suh, Y.C.; McCullough, B.F. Factors Affecting Crack Width of Continuously Reinforced Concrete Pavement. *Transp. Res. Rec.* **1994**, *1449*, 134–140.
6. Zhang, Y.T.; Roesler, J.R. Improved Backcalculation Procedure for Continuously Reinforced Concrete Pavement. *Transp. Res. Rec.* **2018**, *2672*, 336–347. [CrossRef]
7. Zhang, Y.T.; Roesler, J.R.; Huang, Z.Y. A method for evaluating CRCP performance based on edge-loaded FWD test. *Mater. Struct.* **2020**, *53*, 46. [CrossRef]
8. Kim, K.; Han, S.; Tia, M.; Greene, J. Optimization of parameters affecting horizontal cracking in continuously reinforced concrete pavement (CRCP). *Can. J. Civ. Eng.* **2019**, *46*, 634–642. [CrossRef]

9. Kohler, E.; Roesler, J. *Accelerated Pavement Testing of Extended Life Continuously Reinforced Concrete Pavement Sections, Final Report, Transportation Engineering Series No. 141, Illinois Cooperative Highway and Transportation Series No. 289*; University of Illinois: Urbana, IL, USA, 2006; 354p.
10. Eisa, M.; EI-Salakawy, E.F.; Benmokrane, B. Finite Element Model for New Continuous Reinforced Concrete Pavement (CRCP) using GFRP Bars. In Proceedings of the 17th International Conference on Modelling and Simulation, Montreal, QC, Canada, 24 May 2006; pp. 609–616.
11. Chen, H.L.; Choi, J.H.; GangaRao, H.V.; Kopac, P.A. Steel versus GFRP Rebars? *Public Roads* **2008**, *72*, 2–10.
12. Choi, J.H.; Chen, R.H.L. Design of GFRP Reinforced CRCP and its Behavior Sensitivity to Material Property Variations. *Constr. Build. Mater.* **2015**, *79*, 420–432. [CrossRef]
13. Chen, R.H.L.; Choi, J.H. Analysis of Shrinkage and Thermal Stresses in Concrete Slabs Reinforced with GFRP Rebars. *J. Mater. Civ. Eng.* **2011**, *23*, 612–627. [CrossRef]
14. Benmokrane, B.; Eisa, M.; EI-Gamal, S.; EI-Salakawy, E.; Thebeau, D. First Use of GFRP Bars as Reinforcement for Continuous Reinforced Concrete Pavement. In Proceedings of the Fourth International Conference on FRP Composites in Civil Engineering, Zurich, Switzerland, 22–24 July 2008.
15. Benmokrane, B.; Nakouregui, A.S.; Mohamed, H.M.; Thebeau, D.; Abdelkarim, O.I. Design, construction, and performance of continuously reinforced concrete pavement reinforced with GFRP bars: Case study. *J. Compos. Constr.* **2020**, *24*, 05020004. [CrossRef]
16. Gu, X.Y.; Dong, Q. Laboratory test and numerical simulation of bond performance between baslat fiber reinforced polymer rebar and concrete. *J. Test. Eval.* **2012**, *40*, 1148–1155. [CrossRef]
17. Xin, D.; Zollinger, D.; James, R. One-Dimensional Model for Analysis of CRC Pavement Growth. *J. Transp. Eng.* **1992**, *118*, 557–575. [CrossRef]
18. Meng, C.; Cai, L.; Wang, G. An approximate model for continuously reinforced concrete pavement under temperature loading. *ACI Mater. J.* **2019**, *116*, 193–204. [CrossRef]
19. McGhee, K.H. Experience with Continuously Reinforced Concrete Pavements in Virginia. *Transp. Res. Rec.* **1974**, *485*, 14–24.
20. McCullough, B.F.; Zollinger, D.G.; Dossey, T. *Evaluation of the Performance of Texas Pavements Made with Different Coarse Aggregates, Research Report 3925-1*; Center for Transportation Research, the University of Texas at Austin: Austin, TX, USA, 1999.
21. Tayabji, S.D.; Stephanos, P.J.; Gagnon, J.S.; Zollinger, D.G. *Performance of Continuously Reinforced Concrete Pavements Volume II: Field Investigations of CRC Pavements, Report No. FHWA-RD-94-179*; PCS/Law Engineering: Beltsville, MD, USA, 1998.
22. American Association of State Highway and Transportation Officials (AASHTO). *Mechanistic-Empirical Pavement Design Guide: A Manual of Practice, AASHTO Designation: MEPDG-1*; AASHTO: Washington, DC, USA, 2008.

Publisher's Note: MDPI stays neutral with regard to jurisdictional claims in published maps and institutional affiliations.

© 2020 by the authors. Licensee MDPI, Basel, Switzerland. This article is an open access article distributed under the terms and conditions of the Creative Commons Attribution (CC BY) license (http://creativecommons.org/licenses/by/4.0/).